Progress In Electromagnetics Research C, Vol. 33, 185–198, 2012

DESIGN OF PLANAR COUPLED-FED MONOPOLE ANTENNA FOR EIGHT-BAND LTE/WWAN MOBILE HANDSET APPLICATION

C.-H. Ku[1], H.-W. Liu[2, *], and Y.-X. Ding[1]

[1]Department of Electrical Engineering, Ming Chi University of Technology, Tai-Shan Dist., New Taipei City 24301, Taiwan

[2]Advanced Research Center, Auden Techno Corp., Pa-Te City, Taoyuan Hsien 33463, Taiwan

Abstract—In this paper, a planar coupled-fed monopole antenna with eight-band LTE/WWAN (LTE700/2300/2500/GSM850/900/1800/1900 /UMTS) operation for mobile handset device application is proposed. It simply consists of a T-shaped driven strip and a coupled radiating structure, which occupy a small PCB area of $50\,(L)\times 15\,(W)\,\text{mm}^2$. This antenna, which is printed on a 0.4 mm FR4 substrate and fed by a 50-Ω coaxial cable, can provide two wide operating bandwidths covering 697–1012 MHz and 1598–2795 MHz for LTE/WWAN communication systems. A prototype of the proposed antenna is fabricated, tested and analyzed. From the measurement results, nearly omnidirectional coverage and stable gain variation across the desired LTE/WWAN bands can be obtained with the antenna.

1. INTRODUCTION

Due to the rapid growth in communication technology, many future portable devices such as smart phone and laptop computer will possess both the WWAN (Wireless Wide Area Network) and the LTE (Long Term Evolution) functions for real-time voice and data transmission. To this end, a multiband antenna design will be a promising technique for those devices. Recently, numerous antenna designs capable of covering not only the GSM850/900/1800/1900/UMTS bands (824–896/880–960/1710–1880/1850–1990/1920–2170 MHz) but also the LTE700/2300/2500 bands (698–787/2305–2400/2500–2690 MHz) have been proposed and discussed. Considering the design condition

Received 13 August 2012, Accepted 10 October 2012, Scheduled 10 October 2012

* Corresponding author: Hsien-Wen Liu (D9407303@mail.ntust.edu.tw).

in a mobile handset, some antennas with LTE/WWAN operation have attracted very high attention [1–7]. To widen the operating bandwidth, three planar coupled-fed monopole antennas presented in [1–4] were formed with an inductive shorting strip to generate more than three resonant modes. Good multiband property for LTE/WWAN application could be thus obtained with above antenna designs. It was noted that for a smaller mobile handset device, the use of a meander shape was an effective way to reduce the antenna's size. Several internal antennas with a quite compact size were therefore reported in [5–7].

In addition to mobile handset device, many multiband antenna designs [8–13] were suitable to be embedded inside a laptop computer or a tablet computer for LTE/WWAN application. By using a coupled-fed structure to excite the branch radiator, both a loop-type antenna [8] and a shorted monopole antenna [9] could operate at LTE/WWAN bands for a laptop computer. Moreover, there are three useful methods for further expanding the antenna bandwidth, which are based on printed slot [10], parallel resonant circuit [11], and parasitic shorted strip [12]. Above methods all can well assist an internal antenna to attain eight-band feature for laptop computer application. It should be noted that radiation performance is another crucial issue for LTE/WWAN antenna design. A compact multi-branch inverted-F antenna [13], printed on a ceramic substrate with low loss property, may realize good radiation efficiency over the bands of interest. According to those studies shown in [1–13], we clearly know that an internal LTE/WWAN antenna must be designed together with a compact size, multiband operation and good radiation performance for real application.

Regarding the LTE/WWAN application in a mobile handset device, a planar coupled-fed eight-band monopole antenna is proposed and studied in this paper. This design is simple and implemented using a low cost FR4 substrate. It has a compact size of $50\,(L) \times 15\,(W)\,\mathrm{mm}^2$ and two wide operating bandwidths covering 697–1012 MHz and 1598–2795 MHz. By properly forming the coupling structure, the proposed design can well function as an internal antenna for a mobile handset. It is also well-known that this kind of coupling driven-parasitic elements has been found useful for multiband operation with a small size [14]. Details of the antenna design and resonant principle are then described in Section 2. A fabricated prototype of the antenna will be experimentally tested and analyzed in Section 3. Parametric study for further tuning the antenna's property will be performed and discussed as well. Finally, this paper will be concluded with a brief summary in Section 4.

2. ANTENNA DESIGN

Figure 1(a) depicts the whole design structure of the proposed planar coupled-fed eight-band monopole antenna. It is composed of a T-shaped driven strip and a coupled radiating structure, which is

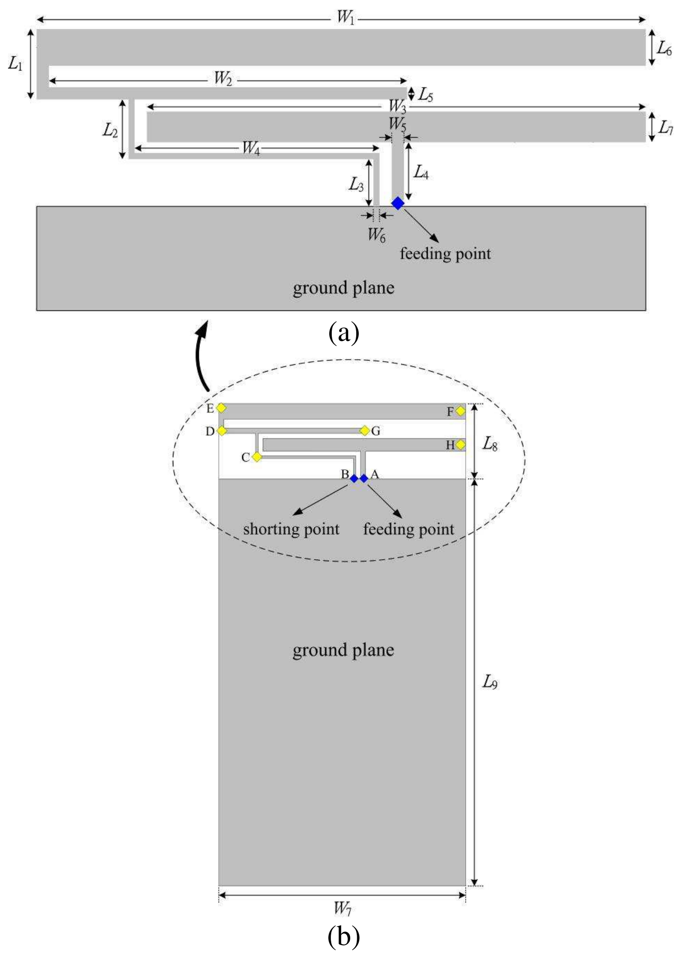

Figure 1. Design structure of the proposed coupled-fed eight-band monopole antenna. (a) Antenna geometry, (b) antenna integrated with the ground plane. ($L_1 = 6$ mm, $L_2 = 5.5$ mm, $L_3 = 3.5$ mm, $L_4 = 5$ mm, $L_5 = 1$ mm, $L_6 = 3$ mm, $L_7 = 3$ mm, $L_8 = 15$ mm, $L_9 = 85$ mm, $W_1 = 50$ mm, $W_2 = 29$ mm, $W_3 = 41.5$ mm, $W_4 = 20.5$ mm, $W_5 = 1$ mm, $W_6 = 0.5$ mm and $W_7 = 50$ mm).

fabricated on a 0.4-mm-thick FR4 substrate with dielectric constant $\varepsilon_r = 4.4$ and loss tangent $\tan\delta = 0.02$. The antenna is fed by a 50 ohm coaxial cable and has a compact size of $50\,(L) \times 15\,(W)\,\text{mm}^2$, so that it can be used inside a mobile handset device as an internal antenna. As shown in Figure 1(b), the antenna is placed at the top edge of the ground plane with a suitable size of $100\,(L) \times 50\,(W)\,\text{mm}^2$. Such ground plane to model a mobile handset device is reasonable for actual application. In order to have the LTE/WWAN eight-band operation, the proposed antenna must be designed with multiple resonant modes. To this end, the antenna utilizes the T-shaped strip to generate 760 MHz mode, and applies the coupled radiating structure to produce 1600 MHz and 2320 MHz modes, respectively. It is noted that the 760 MHz mode can dominate the lower band performance, and the 1600 MHz and 2320 MHz modes can be combined for the upper band operation. Here we employ the full-wave simulator HFSS [15] to model the antenna configuration and also analyze its surface current. Thus the antenna design can be illustrated clearly.

Figure 2(a) shows the current distribution when the antenna is

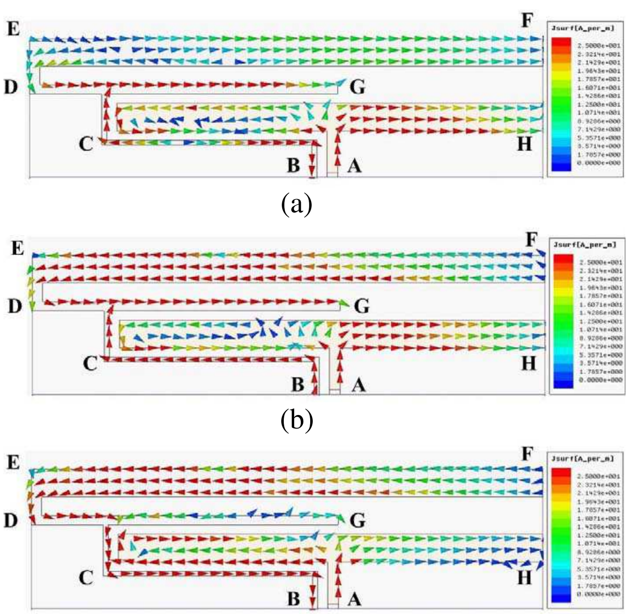

Figure 2. Simulated surface current distributions for the proposed antenna. (a) 2320 MHz, (b) 1600 MHz, (c) 760 MHz.

excited with the frequency of 2320 MHz. It is obvious that strong currents flow along the path A-H (locations are shown in Figure 1(b)), whose length is calculated to be 27 mm and near quarter wavelength of 2320 MHz. This means that the T-shaped strip of the antenna can act as not only a driven strip but also a radiating monopole structure. Figure 2(b) simulates the current trend at 1600 MHz. According to the simulated results, strong and in-phase currents can be generated around the path B-C-G. Note that the path B-C-G is estimated with a length of 47 mm, which also corresponds to quarter wavelength of 1600 MHz. Therefore the path B-C-G is mainly working for the 1600 MHz mode. Moreover, the simulated surface currents at 760 MHz for the antenna are plotted in Figure 2(c), where intense and uniform current distributions can be observed around the path B-C-D-E-F. This is because the path B-C-D-E-F, which has a longest length of 95 mm, is near quarter wavelength of 760 MHz. Three fundamental resonant modes can be thus created with the antenna. Note that good impedance matching across the desired LTE/WWAN bands is also important for the proposed antenna. To successfully produce the lower 760 MHz and 1600 MHz modes, a space between the coupled radiating structure and the T-shaped strip must be carefully evaluated. Then the coupled radiating structure is also connected to the ground plane, where the shorting point B is designed at the left side of the feeding point A. The effect from capacitive coupling can be appropriately

Table 1. Size comparison for the proposed antenna with previous planar designs.

Reference	Antenna Size	Size Reduction Ratio (Proposed/Reference)
[1] Chu and Wong	$60\,(L) \times 15\,(W)\,\text{mm}^2$ ($900\,\text{mm}^2$)	83.3%
[2] Lee and Wong	$40\,(L) \times 12\,(W)\,\text{mm}^2$ ($480\,\text{mm}^2$)	156.3%
[3] Chen and Wong	$60\,(L) \times 10\,(W)\,\text{mm}^2$ ($600\,\text{mm}^2$)	125%
[10] Wong and Lin	$75\,(L) \times 12\,(W)\,\text{mm}^2$ ($900\,\text{mm}^2$)	83.3%
[13] Hu et al.	$96\,(L) \times 11.2\,(W)\,\text{mm}^2$ ($1075.2\,\text{mm}^2$)	69.8%
Proposed design	$50\,(L) \times 15\,(W)\,\text{mm}^2$ ($750\,\text{mm}^2$)	NA

compensated due to above two design considerations.

To completely understand the antenna operation, we also utilize the full-wave simulator, SEMCAD [16], for analyzing the radiation performance and electrical properties of the antenna. The design parameters optimized for the antenna have been eventually determined with $L_1 = 6\,\text{mm}$, $L_2 = 5.5\,\text{mm}$, $L_3 = 3.5\,\text{mm}$, $L_4 = 5\,\text{mm}$, $L_5 = 1\,\text{mm}$, $L_6 = 3\,\text{mm}$, $L_7 = 3\,\text{mm}$, $L_8 = 15\,\text{mm}$, $L_9 = 85\,\text{mm}$, $W_1 = 50\,\text{mm}$, $W_2 = 29\,\text{mm}$, $W_3 = 41.5\,\text{mm}$, $W_4 = 20.5\,\text{mm}$, $W_5 = 1\,\text{mm}$, $W_6 = 0.5\,\text{mm}$ and $W_7 = 50\,\text{mm}$. Since the proposed antenna is planar, we also compare its size with those prior planar designs published in [1–3, 10] and [13]. Comparison results are given in Table 1. It can be seen that the antenna has a medium size. Thus the proposed coupled-fed multiband monopole antenna may be flexibly embedded inside a mobile handset as an internal antenna for LTE/WWAN applications.

3. SIMULATED AND EXPERIMENTAL RESULTS

Figure 3 was a fabricated prototype of the proposed planar coupled-fed eight-band monopole antenna. The prototype was placed at the top edge of the ground plane and fed by a 50 ohm coaxial cable. The antenna's performance was measured by using the vector network analyzer (Agilent ENA E5071B). The simulated and measured return losses were plotted and compared in Figure 4. It can be observed that the simulated and measured results in the lower band have

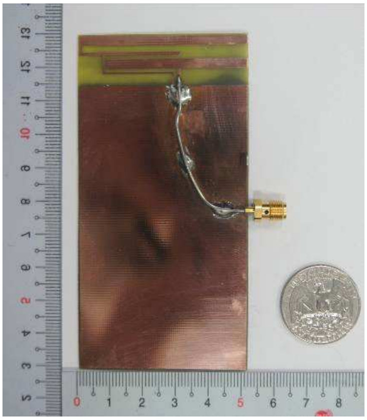

Figure 3. Fabricated prototype of the proposed antenna.

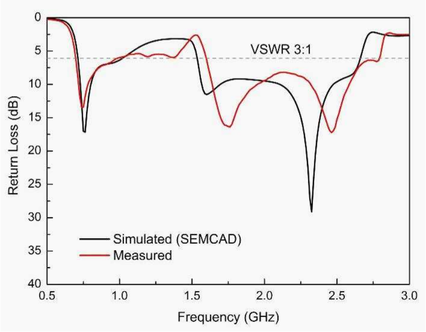

Figure 4. Simulated and measured return losses of the proposed antenna.

good agreement. For the upper band, small discrepancy between the simulations and measurements may be mainly due to the fabrication inaccuracy of the prototype. Note that from the measured results,

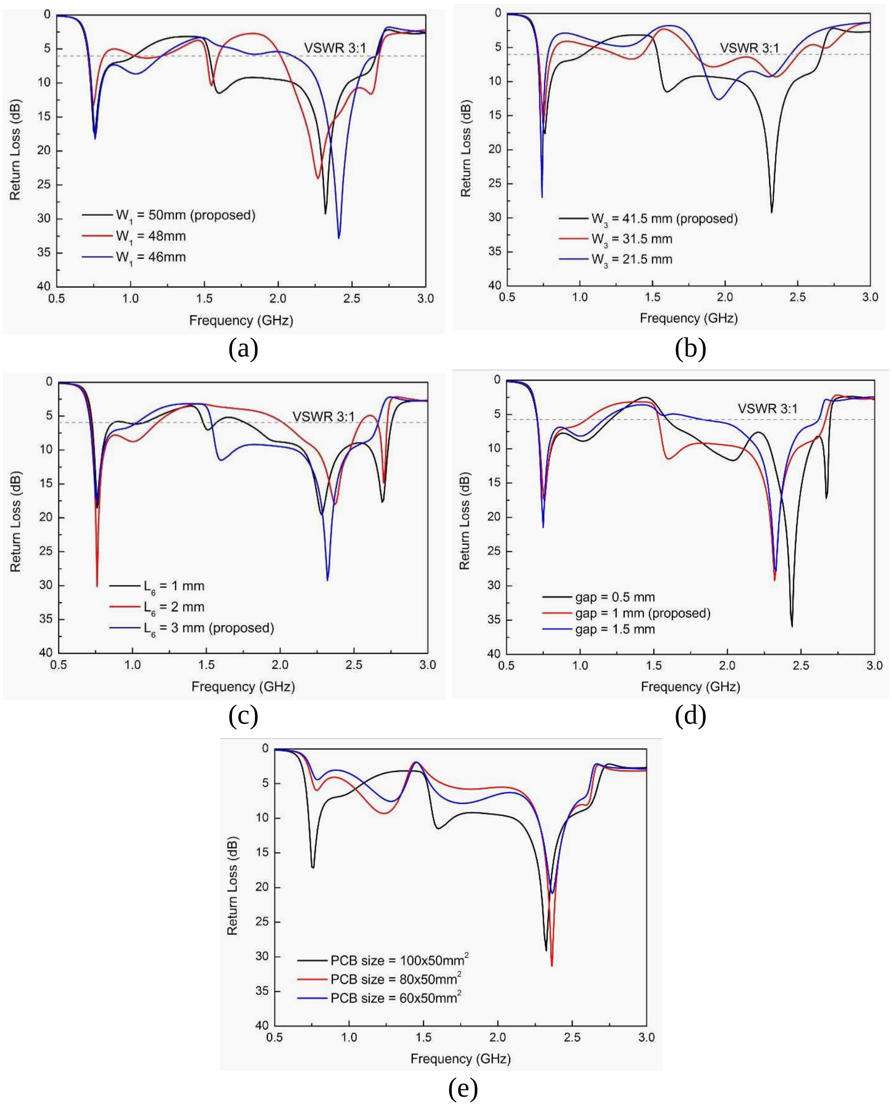

Figure 5. Parametric analysis for the proposed antenna. (a) Parameter W_1, (b) parameter W_3, (c) parameter L_6, (d) gap, (e) PCB size.

however, two distinct resonance modes in the upper band can be still found. This also agrees with the design conception. According to 6 dB return loss (VSWR 3 : 1), two measured impedance bandwidths of the antenna have been determined to be about 697–1012 MHz and 1598–2795 MHz. Thus the desirable eight operating bands, including LTE700/2300/2500 and GSM850/900/1800/1900/UMTS, can be well satisfied with the antenna.

To further understand the antenna's operation, several design parameters to tune the antenna performance are also simulated and investigated. Here we utilize the electromagnetic software package SEMCAD to perform the required simulations. First the parameter W_1 of the antenna design is analyzed with various lengths, as shown in Figure 5(a). It is obvious that the bandwidth of the upper band will be reduced when the W_1 is shortened. Although the parameter W_1 is the end of the path B-C-D-E-F for producing the lower band, it can also adjust the upper band performance. From the simulated results, the $W_1 = 50$ mm is a better choice for our antenna design. Figure 5(b) illustrates the effect from the parameter W_3. It can be seen that as W_3 reduces, both the lower and upper bands will have a narrower bandwidth. This is because the parameter W_3 can dominate the energy coupling intensity from the T-shaped strip to the coupled radiating structure. Note that if W_3 is designed to be 41.5 mm, two wide operating bands can be obtained with the antenna. Therefore the coupling between the driven and parasitic elements plays an important role in determining the bandwidth performance [14, 17].

Figure 5(c) reveals that the antenna performance varies with the parameter L_6. As can be found, while the $L_6 = 2$ mm is utilized for the antenna, the lower band can achieve a larger bandwidth but the upper band has a smaller one. On the other hand, by utilizing the parameter $L_6 = 1$ mm, significant bandwidth reduction and enhancement can be seen in the lower and upper bands, respectively. Referring to the simulated results, proper impedance matching for both the lower and upper bands can be achieved as the antenna operates with the parameter $L_6 = 3$ mm. Moreover, three various gaps between the T-shaped strip and coupled radiating structure are studied in Figure 5(d). It is clear that if the antenna works with the gap = 0.5 mm, the operating bandwidth in the upper band will be reduced obviously. This can be attributed to stronger capacitive coupling. Also, the upper band will shift toward higher frequency when the gap is developed to be about 1.5 mm. Accordingly, better impedance matching can be received as the gap = 1 mm is adopted for the antenna. Moreover, the antenna performance variation against the ground plane size is analyzed in Figure 5(e). It can be observed that when the length of

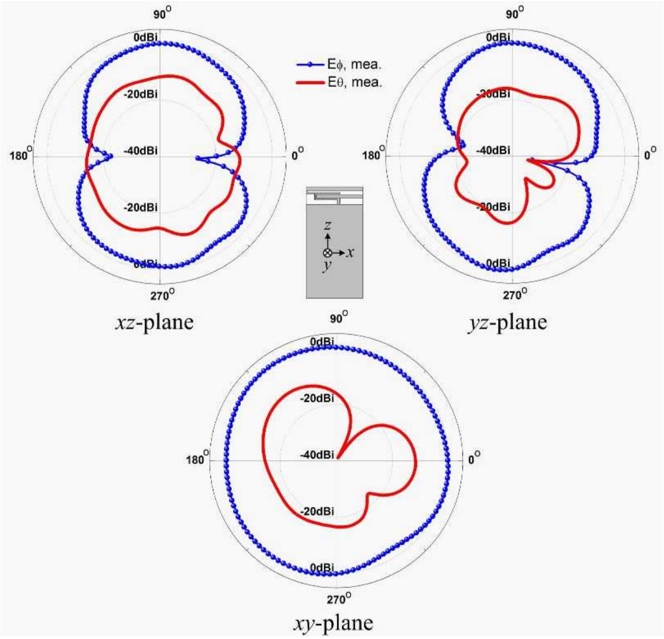

90°
0dBi
-20dBi
-40dBi
180°
0°
270°
Eϕ, mea.
Eθ, mea.
z
x
y
xz-plane
yz-plane
xy-plane

(a)

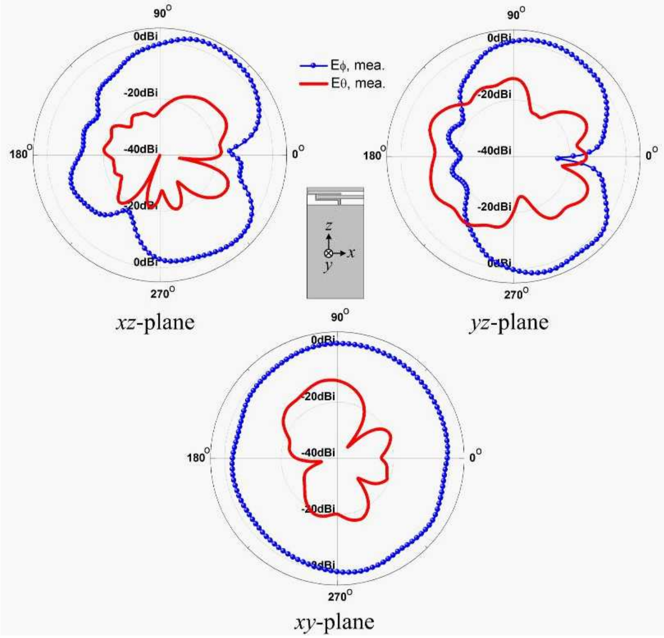

90°
0dBi
-20dBi
-40dBi
180°
0°
270°
Eϕ, mea.
Eθ, mea.
z
x
y
xz-plane
yz-plane
xy-plane

(b)

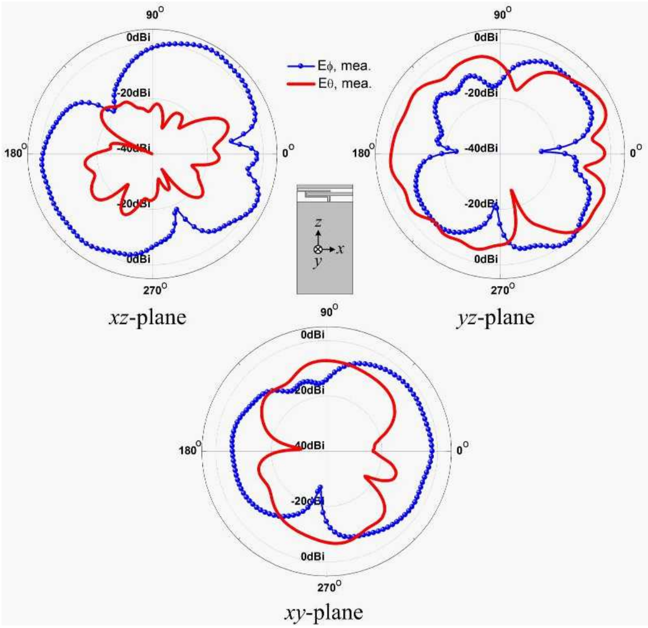

(c)

Figure 6. Measured radiation patterns of the proposed antenna. (a) 780 MHz, (b) 1750 MHz, (c) 2320 MHz.

the ground plane decreases, bandwidth reduction will be happened in both the lower and upper bands. This would result in the proposed antenna unable to meet multiband operation.

Figure 6 illustrates the measured radiation patterns in three typical planes at the frequencies of 780 MHz, 1750 MHz and 2320 MHz for the antenna. For both 780 MHz and 1750 MHz, fairly good omnidirectional pattern and nearly bidirectional pattern can be obtained at the xy-plane and yz-plane, respectively. Referring to the measured results at 2320 MHz, the antenna's patterns in the yz-plane are also close to omnidirectional even though some ripples are included with them. The measured peak gain and antenna efficiency of the proposed design are plotted in Figure 7. Here note that the mismatch loss is included with these measured results. For the lower band, the gain is from 0.95 to 1.62 dBi and the antenna efficiency is around 48–59%, as shown in Figure 7(a). Results in the upper band are given in Figure 7(b), where the gain varies within a range of 2.26–3.67 dBi and the efficiency changes from 51% to 70%. Stable variations for both the gain and efficiency over the desirable LTE/WWAN bands can be

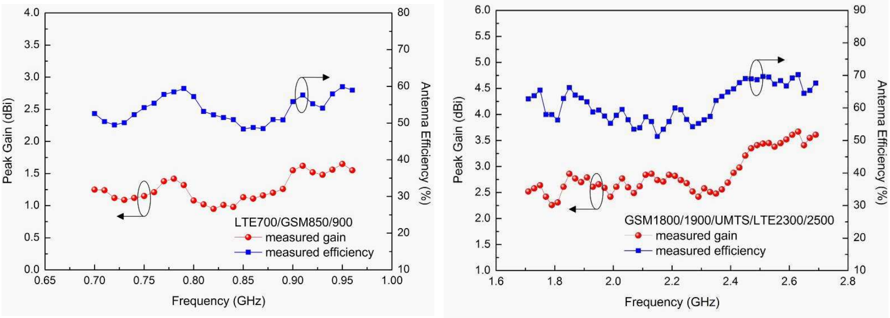

(a) (b)

Figure 7. Measured peak gain and antenna efficiency of the proposed antenna. (a) LTE700/GSM850/900 bands, (b) GSM1800/1900/UMTS/LTE2300/2500 bands.

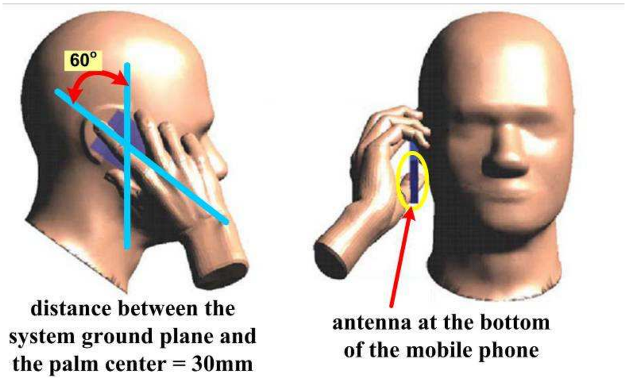

Figure 8. SAR simulation model using head/hand tissues provided by SEMCAD.

hence obtained with the antenna. This would result in an acceptable performance for the antenna used in a LTE/WWAN mobile handset device.

In this work, the SAR (Specific Absorption Rate) results of the antenna are also studied by using the software SEMCAD, where the simulation model is shown in Figure 8. In order to obtain a lower SAR value [18–20], the antenna is positioned at the bottom of the mobile phone. In the figure, the mobile phone is placed with a slant angle of 60°, and the distance between the palm center and system ground plane is reasonably chosen to be 30 mm for testing SAR value. The input power to evaluate the SAR is about 24 dBm for the GSM850/900

Table 2. Simulated 1-g SAR values of the proposed antenna. The return loss shown in the table is the impedance matching level at the testing frequency.

Frequency (MHz)		740	859	925	1795	1920	2045	2350	2595
1-g SAR (W/kg)	head only	0.62	1.28	1.02	1.12	0.78	0.85	0.95	0.55
	head and hand	0.72	1.33	1.14	1.26	0.91	0.88	1.77	1.62
Return loss (dB)	head only	9.8	9.4	8.8	12.3	10.3	11.2	15.2	10.7
	head and hand	10.1	8.6	8.2	14.5	9.9	13.8	12.3	11.6

bands (859 and 925 MHz) and 21 dBm for the GSM1800/1900 bands (1795 and 1920 MHz), UMTS band (2045 MHz), and LTE bands (740, 2350, and 2595 MHz). The simulated SAR values for 1-g head and 1-g head/hand tissues are given in Table 2. The return loss at the testing frequency is indicated as well. Referring to the head only case, the simulated 1-g SAR values across the operating frequencies all satisfy the limit of 1.6 W/kg [21]. When the hand phantom is added for the simulation, the SAR values will increase slightly at 740, 859 and 925 MHz in the lower band. It is also clear that for the upper band, small variations in the SAR values can be seen at frequencies of 1795, 1920 and 2045 MHz. As the testing frequency is set to be 2350 and 2595 MHz, the obtained SAR values are larger than the 1.6 W/kg limit. This is because the hand tissue receives larger power radiated from the antenna. In practical application, the decrease in the SAR values for 1-g head/hand tissue at higher frequencies will be hence required for the proposed antenna.

4. CONCLUSION

A planar coupled-fed eight-band monopole antenna for LTE/WWAN operation has been presented and investigated in this paper. It is simple and has a compact size. By properly designing the T-shaped strip and coupled radiating structure, the antenna can provide three resonance modes to achieve good eight-band feature. Several design parameters to adjust the antenna's performance are also analyzed and discussed. Real radiation performance of the antenna is carefully tested and explained as well. The simulated SAR values for the proposed antenna with the head/hand tissues have been also analyzed. Owing to good coverage and stable gain variation, the proposed internal antenna will be a promising solution for LTE/WWAN mobile handset application.

REFERENCES

1. Chu, F. H. and K. L. Wong, "Planar printed strip monopole with a closely-coupled parasitic shorted strip for eight-band LTE/GSM/UMTS mobile phone," *IEEE Trans. Antennas Propag.*, Vol. 58, No. 10, 3426–3431, Oct. 2010.
2. Lee, C. T. and K. L. Wong, "Planar monopole with a coupling feed and an inductive shorting strip for LTE/GSM/UMTS operation in the mobile phone," *IEEE Trans. Antennas Propag.*, Vol. 58, No. 7, 2479–2483, Jul. 2010.
3. Chen, S. C. and K. L. Wong, "Wideband monopole antenna coupled with a chip-inductor-loaded shorted strip for LTE/WWAN mobile handset," *Microw. Opt. Technol. Lett.*, Vol. 53, No. 6, 1293–1298, Jun. 2011.
4. Wong, K. L. and C. T. Lee, "Wideband surface-mount chip antenna for eight-band LTE/WWAN slim mobile phone application," *Microw. Opt. Technol. Lett.*, Vol. 52, No. 11, 2554–2560, Nov. 2010.
5. Chiu, C.-W., C.-H. Chang, and Y.-J. Chi, "A meandered loop antenna for LTE/WWAN operations in a smart phone," *Progress In Electromagnetics Research C*, Vol. 16, 147–160, 2010.
6. Chen, S. C. and K. L. Wong, "Small-size 11-band LTE/WWAN/WLAN internal mobile phone antenna," *Microw. Opt. Technol. Lett.*, Vol. 52, No. 11, 2603–2608, Nov. 2010.
7. Wong, K. L., M. F. Tu, C. Y. Wu, and W. Y. Li, "On-board 7-band WWAN/LTE antenna with small size and compact integration with nearby ground plane in the mobile phone," *Microw. Opt. Technol. Lett.*, Vol. 52, No. 12, 2846–2853, Dec. 2010.
8. Wong, K. L. and P. J. Ma, "Coupled-fed loop antenna with branch radiators for internal LTE/WWAN laptop computer antenna," *Microw. Opt. Technol. Lett.*, Vol. 52, No. 12, 2662–2667, Dec. 2010.
9. Kang, T. W., K. L. Wong, L. C. Chou, and M. R. Hsu, "Coupled-fed shorted monopole with a radiating feed structure for eight-band LTE/WWAN operation in the laptop computer," *IEEE Trans. Antennas Propag.*, Vol. 59, No. 2, 674–679, Feb. 2011.
10. Wong, K. L. and W. J. Lin, "WWAN/LTE printed slot antenna for tablet computer application," *Microw. Opt. Technol. Lett.*, Vol. 54, No. 1, 44–49, Jan. 2012.

11. Wong, K. L., Y. C. Liu, and L. C. Chou, "Bandwidth enhancement of WWAN/LTE tablet computer antenna using embedded parallel resonant circuit," *Microw. Opt. Technol. Lett.*, Vol. 54, No. 2, 305–309, Feb. 2012.
12. Kang, T. W. and K. L. Wong, "Simple two-strip monopole with a parasitic shorted strip for internal eight-band LTE/WWAN laptop computer antenna," *Microw. Opt. Technol. Lett.*, Vol. 53, No. 4, 706–712, Apr. 2011.
13. Hu, C. L., D. L. Huang, H. L. Kuo, C. F. Yang, C. L. Liao, and S. T. Lin, "Compact multibranch Inverted-F antenna to be embedded in a laptop computer for LTE/WWAN/IMT-E applications," *IEEE Antennas Wireless Propag. Lett.*, Vol. 9, 838–841, 2010.
14. Risco, S., J. Anguera, A. Andújar, A. Pérez, and C. Puente, "Coupled monopole antenna design for multiband handset devices," *Microw. Opt. Technol. Lett.*, Vol. 52, No. 10, 359–364, Feb. 2010.
15. Ansoft Corporation HFSS [Online]. Available: http://www.ansoft.com.
16. SEMCAD, Schmid & Partner Engineering AG (SPEAG) [Online]. Available: http://www.semcad.com.
17. Anguera, J., C. Puente, C. Borja, G. Font, and J. Soler "A systematic method to design single-patch broadband microstrip patch antennas," *Microw. Opt. Technol. Lett.*, Vol. 31, No. 3, 185–188, Nov. 2001.
18. Li, C. H., E. Ofli, N. Chavannes, and N. Kuster, "Effects of hand phantom on mobile phone antenna performance," *IEEE Trans. Antennas Propag.*, Vol. 57, 2763–2770, 2009.
19. Hsu, M. R. and K. L. Wong, "Seven-band folded-loop chip antenna for WWAN/WLAN/WiMAX operation in the mobile phone," *Microw. Opt. Technol. Lett.*, Vol. 51, 543–549, 2009.
20. Lee, C. T. and K. L. Wong, "Internal WWAN clamshell mobile phone antenna using a current trap for reduced groundplane effects," *IEEE Trans. Antennas Propag.*, Vol. 57, 3303–3308, 2009.
21. American National Standards Institute (ANSI), "Safety levels with respect to human exposure to radio-frequency electromagnetic field, 3 kHz to 300 GHz," ANSI/IEEE Standard C95.1, Apr. 1999.